

# Modelling Loran-C Envelope-to-Cycle Differences in Mountainous Terrain

Dr. Paul Williams and Prof. David Last  
University of Wales, Bangor, UK

## Abstract

The potential for using Loran-C for land vehicle tracking and marine and aeronautical navigation in a hybrid combination with GNSS is well recognised in this *post-Volpe Report* era. But to get the best accuracy, integrity, and availability from a Loran receiver we need as much information as possible about the signal. For example, knowing the Additional Secondary Factor (ASF) values allows the highest absolute accuracy to be obtained. Similarly, foreknowledge of the Envelope-to-Cycle Differences (ECDs) of the received signals helps the receiver identify the tracking points, or the individual cycles, of the Loran-C pulses. This clearly minimises cycle slips and maximises integrity.

The authors have recently worked with the US Federal Aviation Administration (FAA) in a programme designed to model Loran field strengths, ASFs, and ECDs. The computer models developed employ Monteath's method to calculate the attenuations and delays of Loran signals, taking into account not only conductivity variations along the propagation paths but also any irregular terrain. This approach has been used to produce field strength and ASF maps for various regions of the US, examples of which will be shown in the paper.

When it comes to computing the ECDs of *received* pulses, Monteath's method also lets us estimate the effects of attenuation and delay on the individual frequency components of the Loran signals across the band 90-110 kHz, and so establish pulse shapes. We then encounter an interesting problem: how to compute the ECDs of these distorted pulses. It appears that the various well-established methods for calculating ECD values are designed only for use with transmitted pulses of variable ECD, but perfect shape.

The paper demonstrates how we predict the shapes of received pulses and discusses the problem of translating the results into ECD values. It shows how ECD maps have been produced for the FAA programme, using a Group Delay method proposed by Peterson.

## 1 Introduction

For a number of years now, the present authors have been developing sophisticated methods for modelling Loran-C Additional Secondary Factors (ASFs). Using the most accurate databases available of ground conductivity [1], coastline [2] and terrain elevation [3], they have successfully predicted ASFs for NELS (the North West

European Loran System) out to 1000km from each transmitter. The datasets produced are publicly available.

Now, by taking the original software for modelling ASFs, and adding extra functionality, we show that it is possible to model Loran Envelope-to-Cycle Difference (ECD) values.

## 2 Envelope to Cycle Difference (ECD)

At a superficial level, ECD is straightforward to understand, but the underlying mechanisms that cause ECD to change as a signal propagates are complex. Fig. 1 shows a Loran-C transmitted pulse.

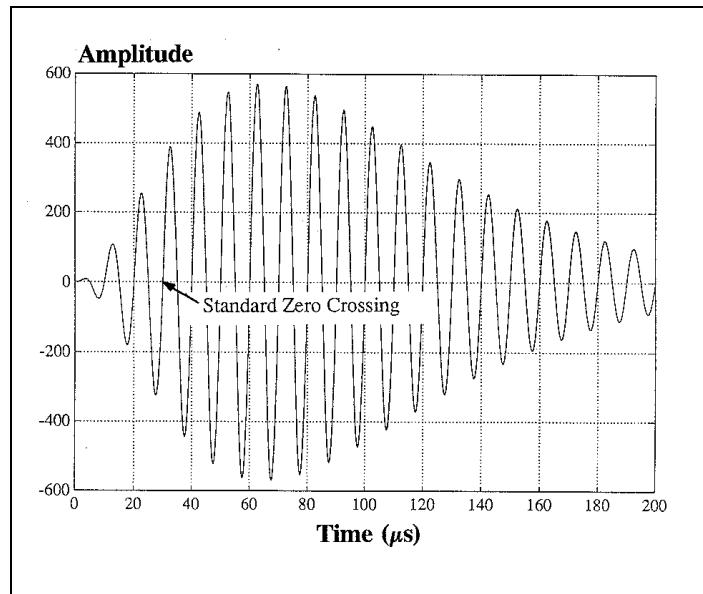


**Fig. 1 - The Loran-C pulse.**

The equation that describes it is:

$$i(t) = A(t - \tau)^2 e^{\frac{2(t-\tau)}{65}} \sin(0.2\pi t + PC),$$

where  $A$  is a scale factor,  $t$  is time,  $\tau$  is ECD and  $PC$  is the phase code.

The standard zero crossing, the point traditionally tracked by receivers, comes 30 $\mu$ s after the start of the pulse. The receiver tries to identify that specific positive-going zero crossing by reference to the envelope of the pulse.

Fig. 2(a) shows the leading edge of the envelope. The receiver is required to find the point on the envelope at which the slope, Fig. 2(b), corresponds to that at the 30 $\mu$ s point this point is termed the *Envelope Tag Point*, or *Tracking Point*. The envelope is, of course, a fiction –an imaginary line joining together the peaks of the cycles. So, in practice, the receiver measures the amplitudes of the half-cycle peaks and look for

two adjacent ones that have the right ratio. Mid-way between them lies the zero-crossing.

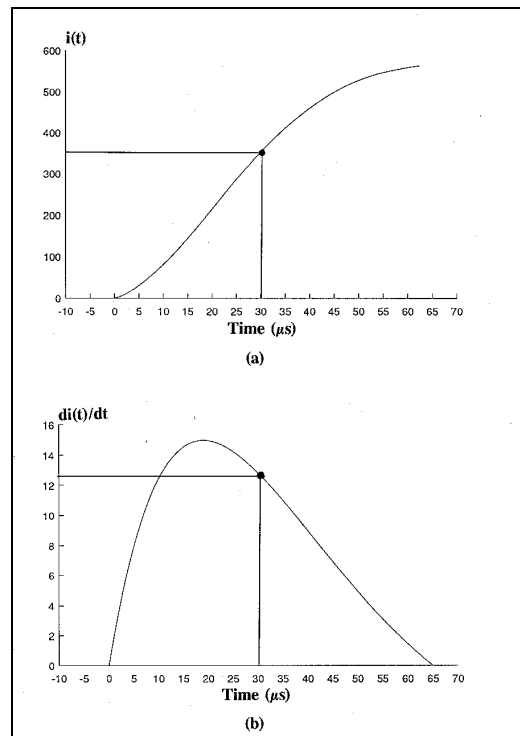


**Fig. 2 – Loran-C pulse envelope leading edge.**

If, however, the shape of the envelope is incorrect, or the envelope has moved with respect to the zero-crossings, this envelope tracking point no longer lines up with the standard zero-crossing. The difference between the two is the envelope-to-cycle difference, or ECD. This explanation describes a simple form of signal tracking, as employed by relatively primitive receivers; nevertheless, the principle also applies to any more sophisticated modern receiver that uses the envelope to find zero-crossing points.

Fig. 3 illustrates a standard Loran pulse, plus two others in which the envelope is  $2.5\mu\text{s}$  early and  $2.5\mu\text{s}$  late, respectively. An early envelope is deemed, quite arbitrarily, to correspond to a negative ECD, and a late one positive. Since most receivers select the nearest zero-crossing to the envelope tracking point detected, they can tolerate up to  $5\mu\text{s}$  ECD error in either sense. An ECD error greater than this would cause the receiver to track the wrong zero-crossing. There would then be a serious error in the measured position; the receiver would be said to have suffered a *cycle slip*. So, ECD is an important factor in the design and proper functioning of receivers.

The ECDs of transmitted pulse are carefully monitored and controlled [4]. But noise and interference can affect the ECD of the received signal. These effects are reduced by receivers' averaging large numbers of pulses. Synchronous interference, however, can still affect the ECD; such interference is minimised, especially in Europe, by means of notch filters or signal processing.

ECD also changes as signals propagate over sea-water, and more rapidly if they travel over land. The shift is in the negative direction; that is, the cycles progressively lag the envelope.

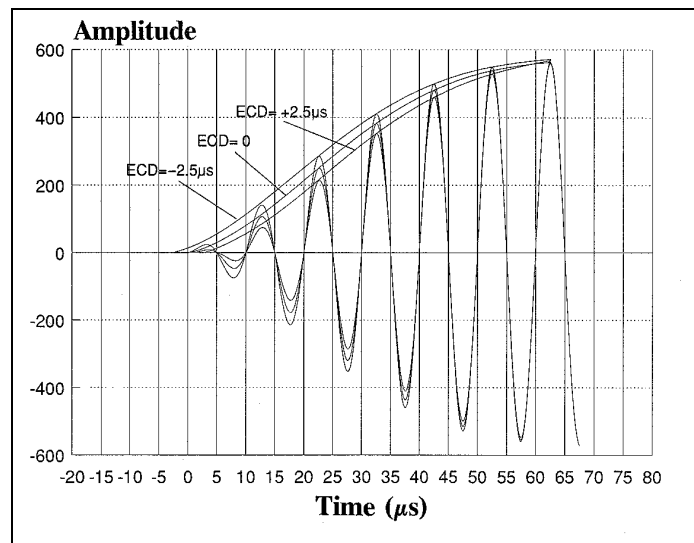


**Fig. 3 – Pulses with ECD values of  $-2.5\ \mu\text{s}$ , zero, and  $+2.5\ \mu\text{s}$ .**

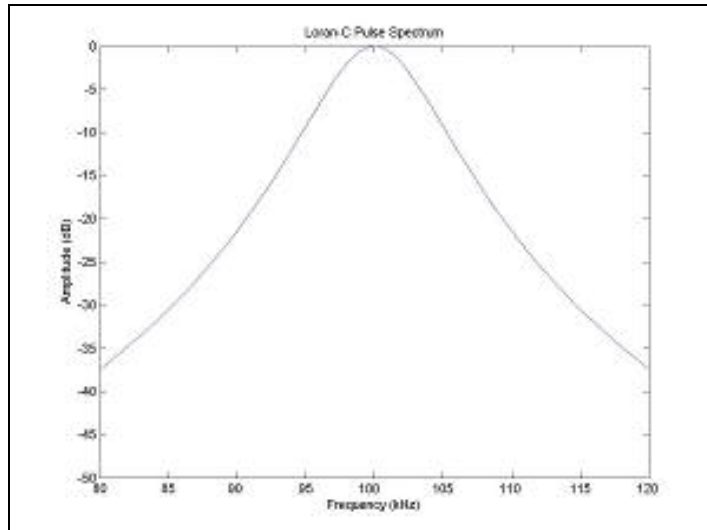
### 3 The Cause of ECD Shifts as Signals Propagate

Fig. 4 shows the spectrum of a standard Loran-C pulse. The velocity of propagation changes slightly with frequency across this range. Thus, some Loran components travel faster than others. As a result, the speed at which the cycles travel (the phase velocity) is different from the speed of the envelope (the group velocity). The result is a change in ECD.

But that is only part of the story. Not only the velocities of the signal components but also their amplitudes vary with frequency, especially over land. Both do so in a complex way. So, the pulse becomes distorted, which contributes a further component of ECD change.

### 4 Modelling ECD values

A number of simple approximations to the change of ECD with distance have been developed. In 1961, the US Coast Guard first examined these mechanisms and estimated theoretically that the change of ECD should be about  $3\ \mu\text{s}$  per 1000 nautical miles (NM) of sea-water [5]. A US Department of Transportation measurement campaign in the late 1970s led to a modified figure of  $2.5\ \mu\text{s}$  per 1000NM. By analysing the same data Dean showed that in mountainous terrain there could be dramatic ECD shifts of up to  $4\ \mu\text{s}$  over relatively short distances. These large shifts often recovered once the signals had left the mountains behind [6].



**Fig. 4 – Spectrum of the Loran-C pulse ; 99% of energy lies between 90 and 110kHz.**

Sherman examined rates of ECD change with distance over seawater and over land of different values of ground conductivity [7]. The result of his analysis is Sherman's curve (Fig. 5). This was incorporated into the Loran-C model created by Farnworth in the early 1990s [8]. He and Last employed it extensively to model ECD variations in North-West Europe; the results for the station at Ejde, Faroe Islands, are presented in Fig. 6. They show that, even over land of exceptionally low conductivity such as the mountains of Norway, the ECD shift remains within the  $5\mu\text{s}$  limit for as far as the field strengths exceed the minimum acceptable to receivers.

In 1992, Peterson and Dewalt analysed data collected in flight trials performed by Bendix-King [9]. Their curve is plotted, and compared with that of Sherman, in Fig. 5. The rates of change of ECD with distance they established were lower, over both sea-water and most kinds of land except those of the lowest conductivities, than Sherman's. They ascribed the variations in their curve for land of conductivities between  $10^{-3}$  and  $10^{-2} \text{ Sm}^{-1}$  to their using an insufficiently large data sample.

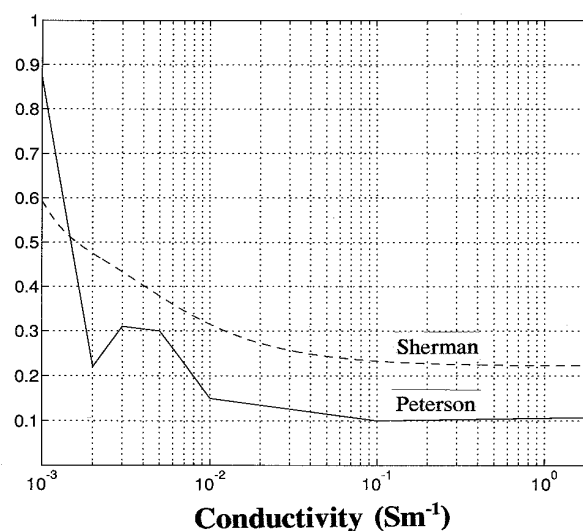


**Fig. 5 – Sherman's curve (dashed) and Peterson's curve (solid).**

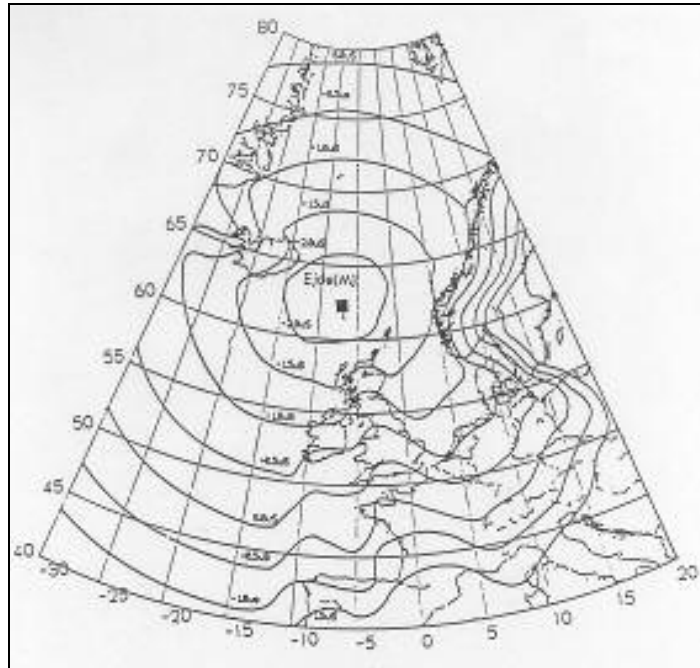


**Fig. 6 – ECD contours around Ejde, Faroe Islands, plotted by earlier technique based on Sherman's curve.**

The discrepancies between Sherman's and Peterson's results may in part be due to the fact that both authors had been obliged to extract ECD rates for different kinds of land from signals that had travelled over mixed paths of differing conductivity. Also, neither could separate the effects of conductivity from those of topography; Peterson recognised that the variations he observed at low conductivity could well be due to terrain effects along his test path caused by mountains near Santa Barbara, California.

Underlying both authors' curves, however, is the assumption that ECD changes steadily with distance over paths of uniform ground conductivity. But is that the case? Research has shown that signal attenuation does *not* change steadily, nor does phase delay. Since these are the principal factors that *cause* ECD change, why should ECD do so? And the presence of mountains along the propagation path makes the problem even more complicated! Clearly, a different approach is needed to analysing ECD variations.

#### **4.1 Modelling ECD Values – A New Approach**

Over a number of years, the present authors have developed models to predict the variations in Loran-C Field Strengths and Additional Secondary Factors (ASFs) along a variety of types of path [10-14]. At first, these employed curves published by the US National Bureau of Standards that related the signal attenuation, and the phase velocity of the Secondary Factor, to range [15]. For paths that had sections of different conductivities, the overall attenuation was estimated using Millington's method [16], and the phase delay by the Millington-Presssey technique [17]. The software developed employed a map of ground conductivity values held in the

computer as a database. The attenuation values were then employed to compute field strengths, and the phase delay values to compute ASFs. A smooth earth was assumed.

Later, it became possible to include the effects of mountains in the calculations. Specifically, the Monteath Method was implemented [18]. Monteath solves propagation equations proposed by Johler & Berry [19]. The resulting computational models determined signal strength and ASF variations using databases of both conductivity and land height. This approach is currently being employed on behalf of the US FAA. Fig. 7 shows an ASF map produced in this way for a region surrounding Grand Junction, Colorado; the Loran station is at Gillette, some 600km to the north-north-east. Fig. 8 shows the corresponding field strength map.

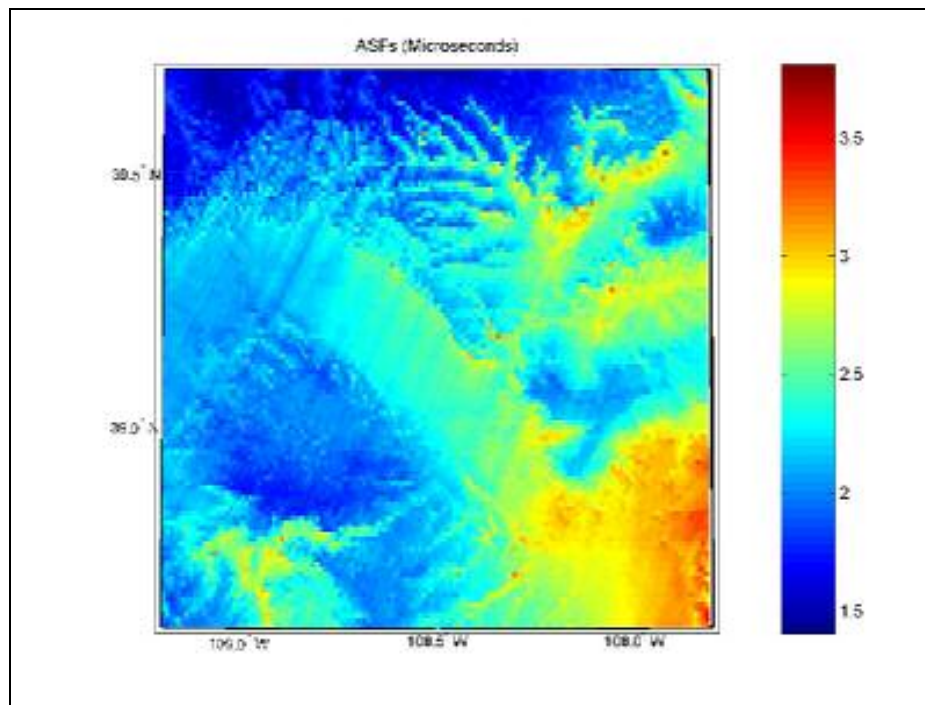


**Fig. 7 – ASF map of Gillette signals around Grand Junction, Colorado.**

## **4.2 The ECD computation method**

Fig. 9 shows how this method may form the basis of a technique to compute ECD values. An ideal Loran-C pulse is generated, with zero ECD (right-hand side of the diagram), and broken down into a number of frequency components using a Fast Fourier Transform. The amplitude and phase of each component are modified by a complex attenuation factor that describes the effect on it of having propagated from the transmitter to the receiver. The received pulse is then assembled from these modified components using an Inverse Fourier Transform, and its ECD calculated by means of a Half-Cycle Peak Ratio (HCPR) algorithm.

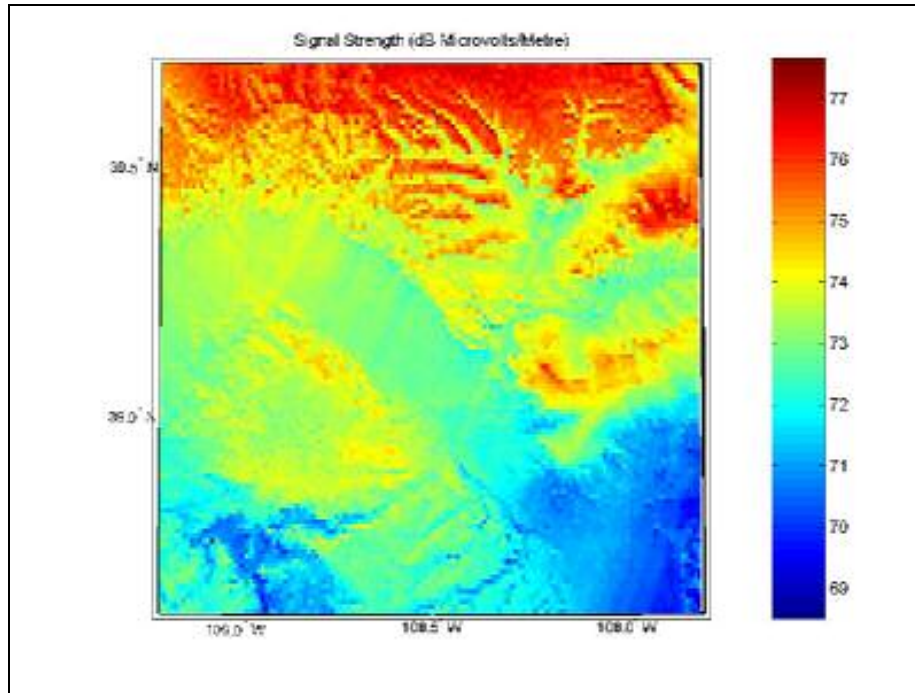


**Fig. 8 – Field strength map of Gillette signals around Grand Junction, Colorado .**

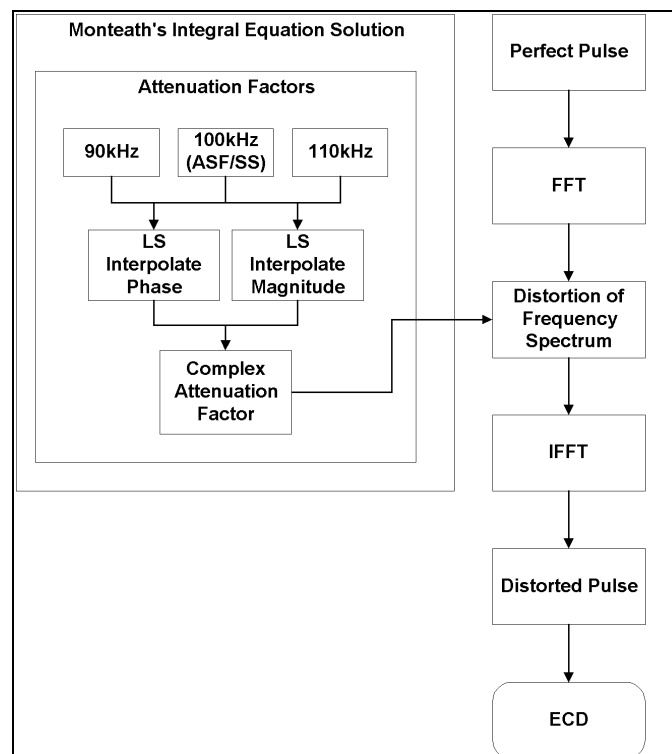


**Fig. 9 – Overview of the ECD computation technique.**

The left-hand side of Fig. 9 shows the method used to establish the complex attenuation coefficient of the propagation path. Working from the conductivity and terrain databases, the software generates a profile of conductivities and terrain elevations at discrete intervals along the transmitter-receiver path; a coastline database ensures that any land-sea transitions are at the right points. It then employs

Monteath's Method to calculate, at each of these discrete points along the path, the magnitude and phase of the complex attenuation factor there. Monteath's Method uses the integral equation shown in Fig. 10.

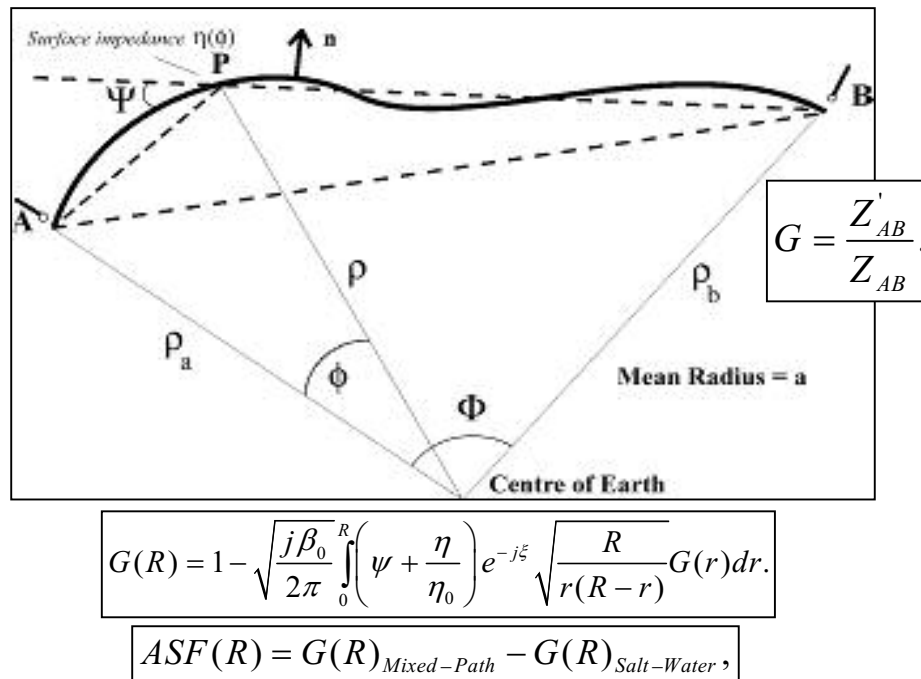


**Fig. 10 – Monteath's Method.**

Sets of complex attenuation factors are computed in this way at each of three frequencies: 90, 100 and 110kHz; this frequency range encompasses 99% of the Loran signal's energy. Then, the values at the frequencies of the individual Fourier components are determined by the technique of Linear Least Squares interpolation between them.

Figs. 11 and 12 illustrate the significance of the amplitude and phase, respectively, of these complex attenuation factors. The signal travels over a 630km-long path from the Loran station at Gillette, Wyoming, to a point south east of Grand Junction, Colorado. This path crosses some exceptionally mountainous terrain; a map displaying the path is shown in Fig. 13 and the terrain elevation is also plotted in Figs. 11 and 12. Fig. 11 shows the magnitude of the attenuation factor of the earth's surface, relative to that at the transmitter, computed at intervals of 630m. As the signal propagates away from the transmitter the attenuation increases, the attenuation being greater at 110kHz than at 90kHz. Fig. 12 shows the corresponding phase delay variations.

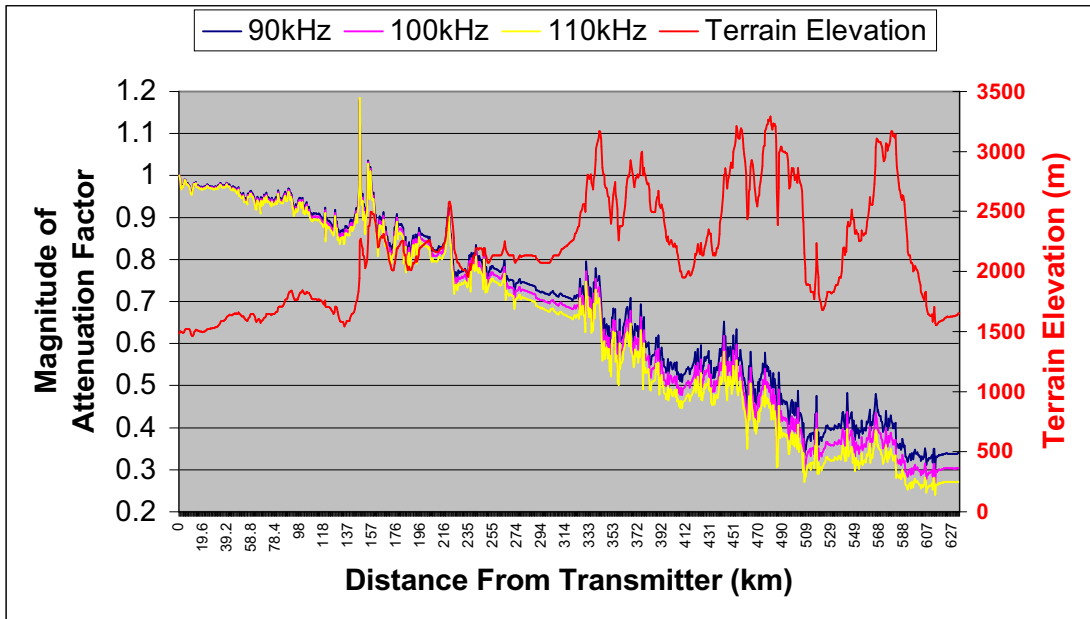


**Fig. 11 – Magnitude of the attenuation factor relative to that at the transmitter along path from Gillette to near Grand Junction.**

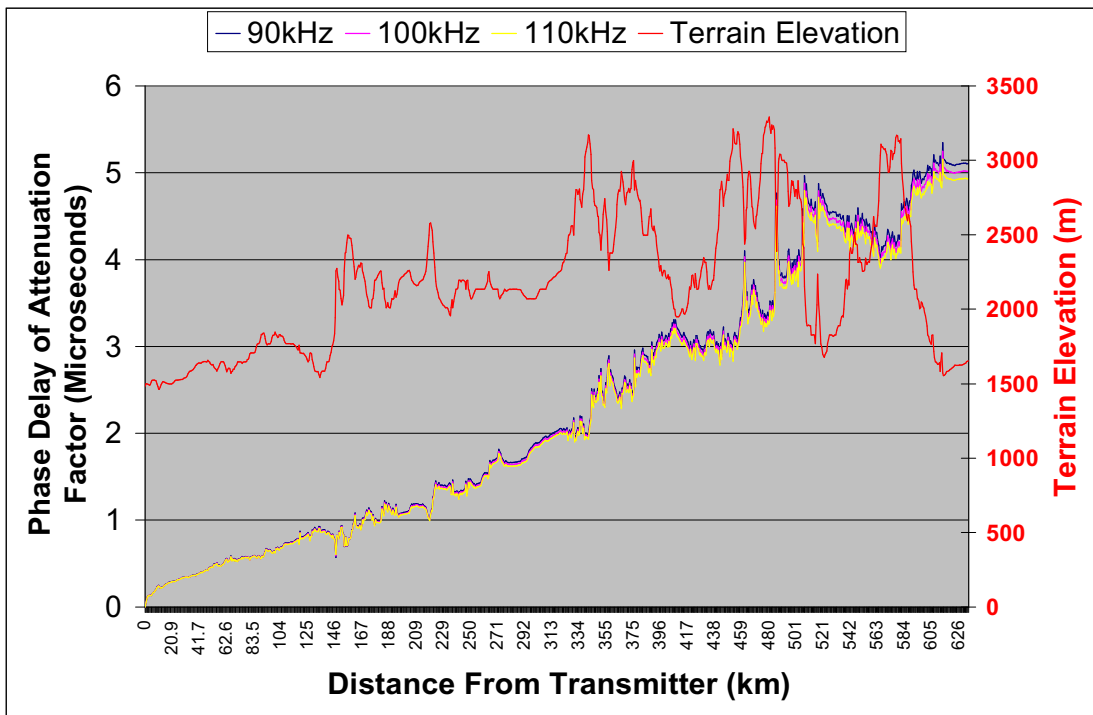


**Fig. 12 – Phase of the attenuation factor along path from Gillette to near Grand Junction.**



**Fig. 13 – Propagation path from Gillette, WY, to near Grand Junction, CO.**

#### **4.2.1 The HCRP Method**

Figs. 14, 15 and 16 illustrate the effect of propagation on a transmitted pulse as modelled by our software. The propagated and distorted pulse (Fig. 15) is reconstructed from the attenuated spectrum (Fig 14). We then compute the Half Cycle Peak Ratio (Fig. 16) and use the ratio value at the  $30\mu\text{s}$  point of the propagated pulse to locate the time with the equivalent ratio on the perfect pulse. The difference between that time and the  $30\mu\text{s}$  point is the ECD.

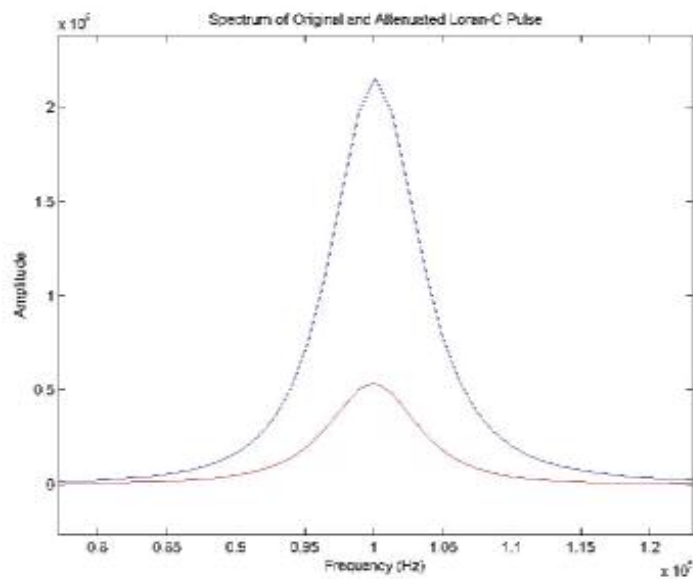


**Fig. 14 – Spectrum of original (blue) and distorted (red) pulses.**

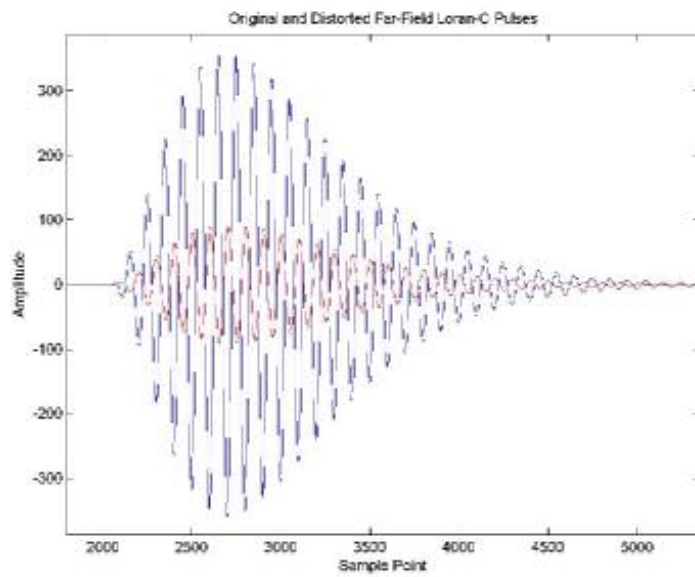


**Fig. 15 – Original pulse (blue) and pulse reconstructed from spectrum after propagation (red).**

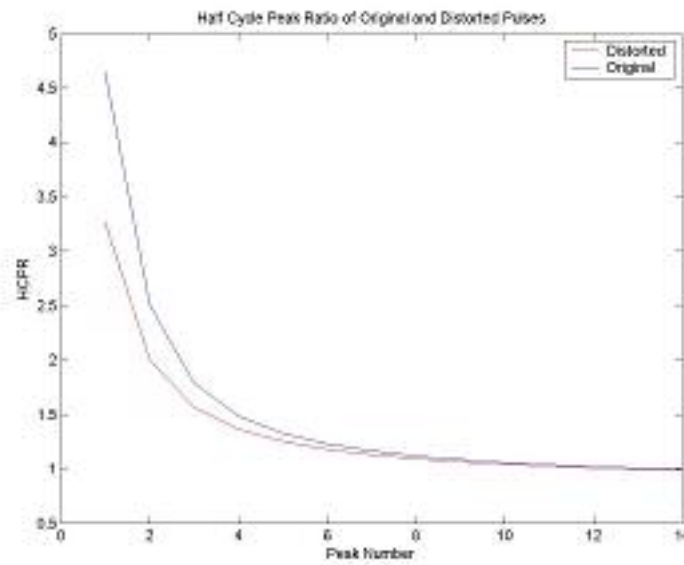


**Fig. 16 – Half Cycle Peak Ratio (HCPR), or envelope, of original (blue) and distorted pulse (red).**

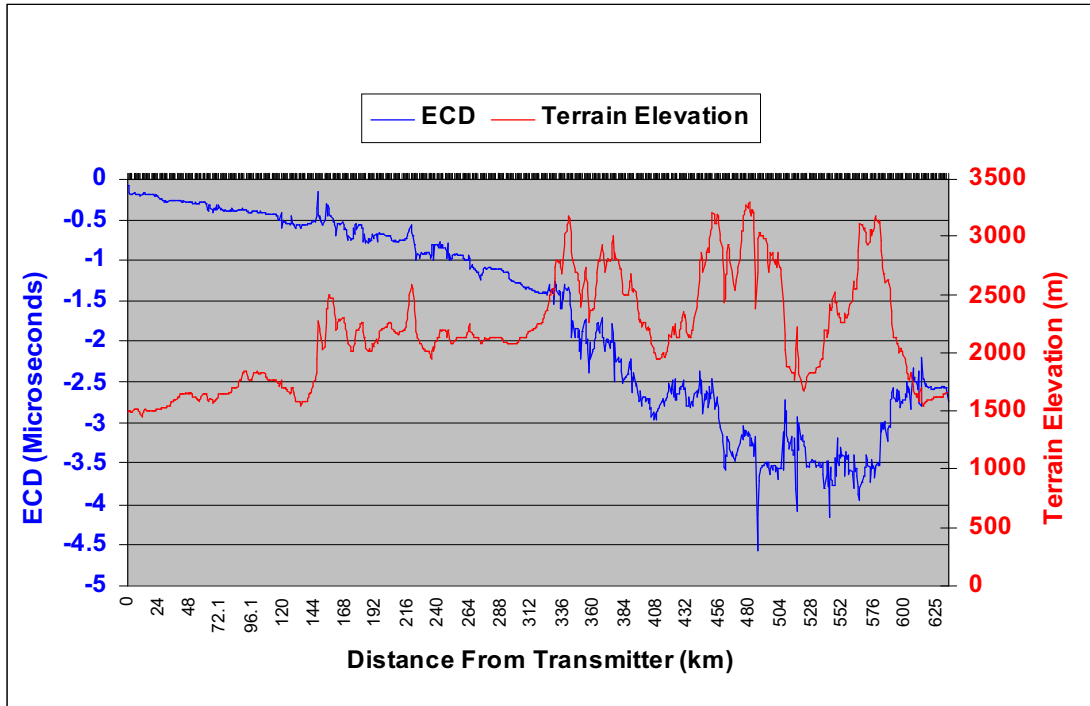


**Fig. 17 – Profile of ECD with distance from the transmitter.**

## 5 ECD Results

### 5.1 Preliminary Results

Using the same profile as earlier, Fig. 17 shows a plot of the ECD shifts, in microseconds. The ECDs change in the correct direction, getting progressively more negative, as the signal propagates away from the transmitter. The rate of change is, as expected, slower over ground of higher conductivity. However, the plot shows a bigger ECD change than anything seen in reality!

### 5.2 Alternative Methods

#### 5.2.1 The USCG Transmitted Pulse Method

As an alternative to the HCPR technique used to produce the results of Fig. 17 we investigated adapting the method used by the United States Coast Guard (USCG) when measuring ECD values at the feed-points to antennas. The principle (Fig. 18) is based on adjusting the amplitude and ECD of the equation that describes the Loran pulse until a best fit is achieved to the distorted received pulse [20]. The resulting ECD value is then extracted from the equation. Unfortunately, the technique involves matching the early peaks of the pulse; these peaks get strongly attenuated during propagation.

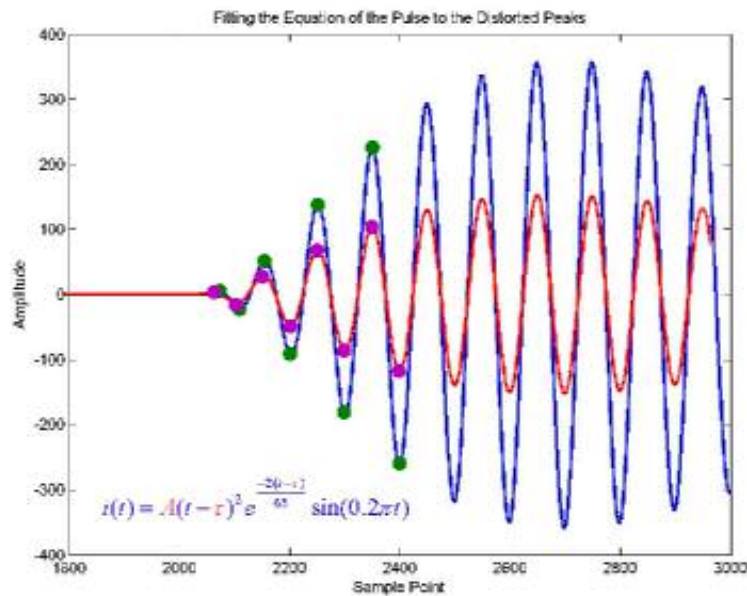


**Fig. 18 – USCG method for determining ECD of transmitted pulse.**

### 5.2.2 Group Delay Method

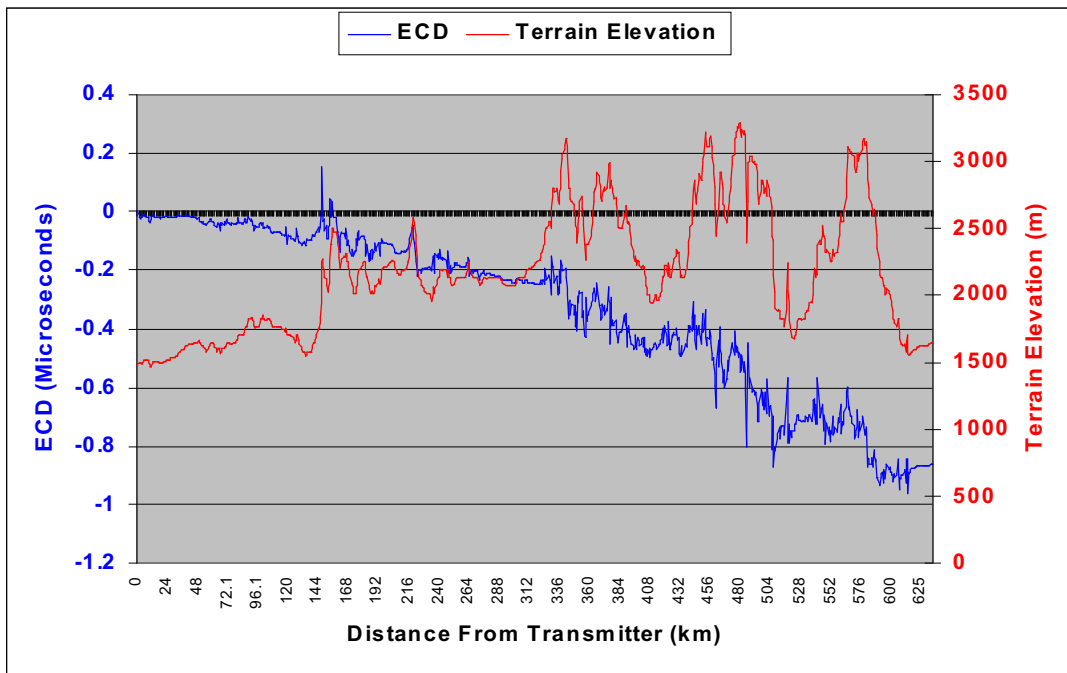
Peterson has proposed an alternative method of determining the ECD of a received pulse. Since the group delay causes the envelope shift, he suggested estimating the ECD from the group delay. He proposed using our software to generate, at each point, the attenuation factors at 90 kHz and 110 kHz, then using the following equation:

$$ECD = 5 \times (\varphi_{110} - \varphi_{90}),$$

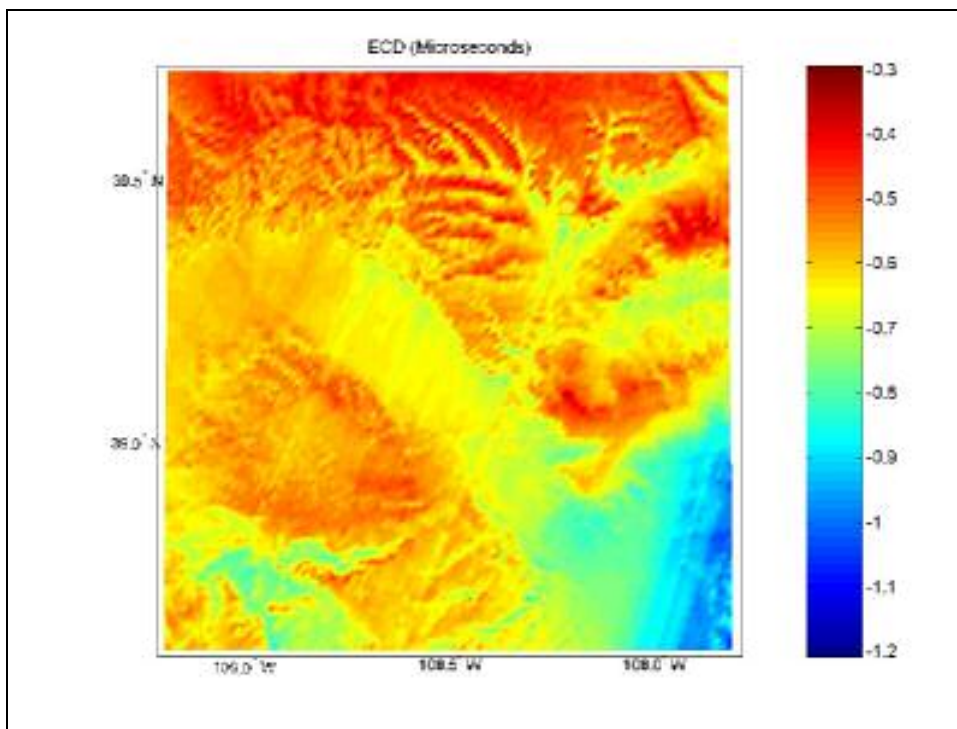
where  $\varphi_{110}$  and  $\varphi_{90}$  are the phase delay, in microseconds, at 110kHz and 90kHz, respectively.

Fig. 19 shows the resulting plot. The ECD falls by about  $0.9\mu\text{s}$  over the 700km path. This is now much more plausible, the results agreeing well with the value of  $0.8\mu\text{s}$  given by Peterson's curve (Fig. 5). This group delay method was used to produce the ECD delivered to the FAA programme (eg Fig. 20).

Figs. 19 and 20 show ECD *changes*, not ECD *values*. It is normal practice to set up transmitters to radiate a positive ECD, commonly  $+2.4\mu\text{s}$ . This is done so that the ECDs will be closest to the ideal value of zero at the edge of coverage where the field strength and signal-to-noise ratio. This maximises receivers' ability to identify the correct zero-crossing under the most difficult conditions. These transmitted ECD values will be built into the computer model.



**Fig. 19 – Modelled ECDs using group delay method.**



**Fig. 20 – ECD map of Gillette signals around Grand Junction, Colorado .**

### **5.3 The Reason for Different Approaches to ECD**

The USCG define the ECD at the base of the antenna but there is no standard definition of the ECD of a received pulse. It is technically difficult to apply techniques such as HCPR and equation fitting to received pulses because the early

peaks may be severely attenuated. The group delay method overcomes these problems by computing an “ECD like” parameter for a propagated pulse. However, it ignores certain factors such as the frequency dependence of attenuation.

The ECDs of received, distorted, pulses are difficult to analyse and model. The change in ECD from the transmitted value is caused by non-linear, frequency-dependent, variations of attenuation and phase velocity across the spectrum of the Loran-C pulse. Both these factors also vary non-linearly with distance from the transmitter, with terrain elevation, and with ground conductivity, and it is necessary to deal with the sum of their effects. So there are additional factors that should, ideally, be incorporated into the model.

## 6 Pulse Shape

It may be more valuable to predict and publish the **shape** of the received pulses rather than their ECD values. Our computer model can do just that.

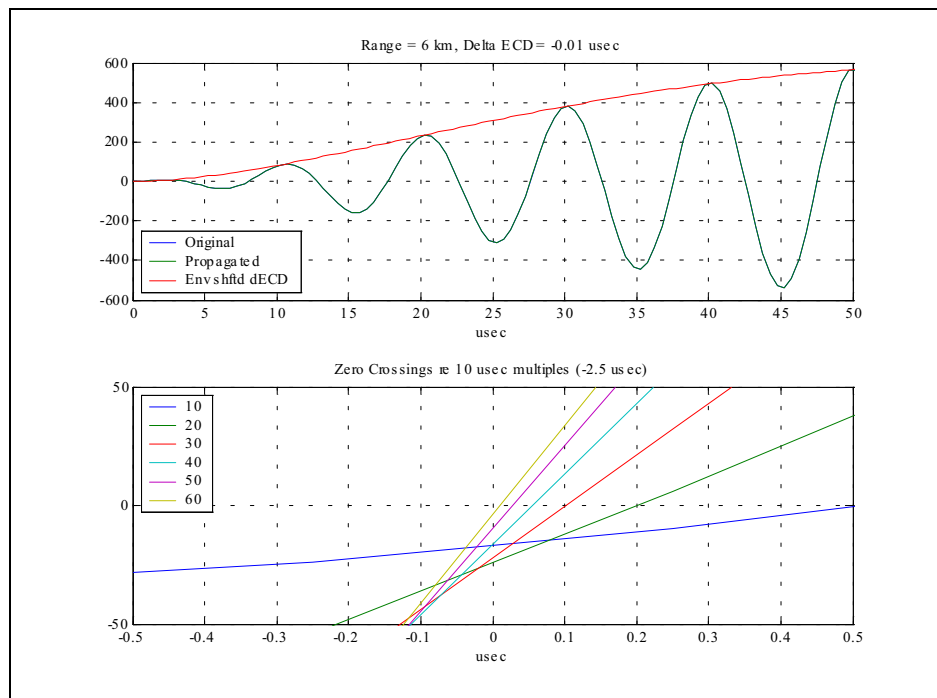


**Fig. 21 – First six positive-going zero crossings of a pulse.**

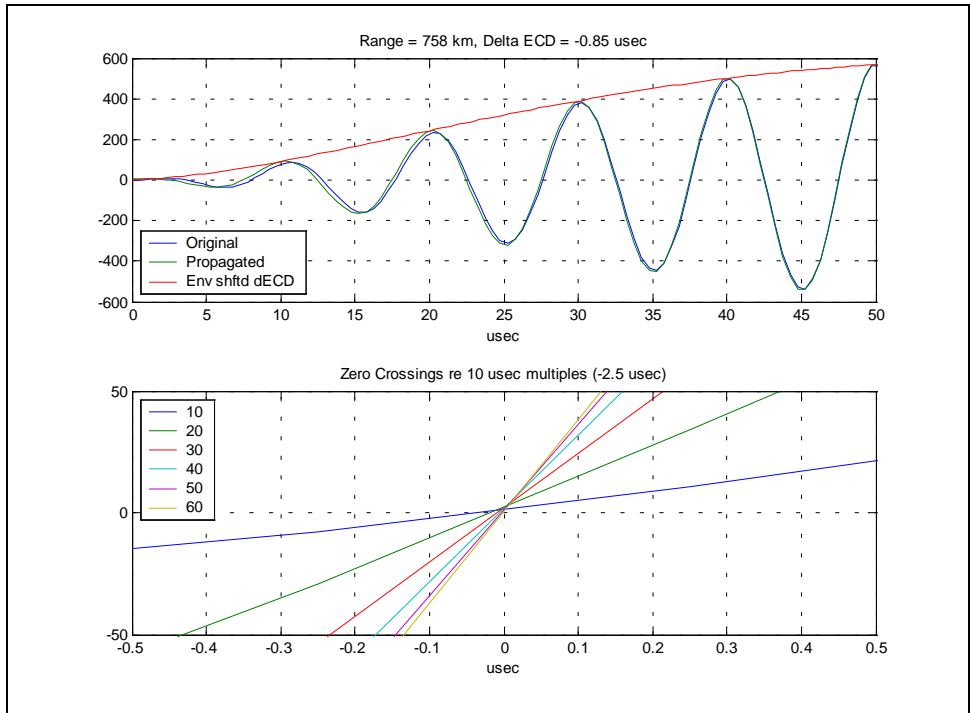


**Fig. 22 – Zero crossings are more equally spaced after 758km.**

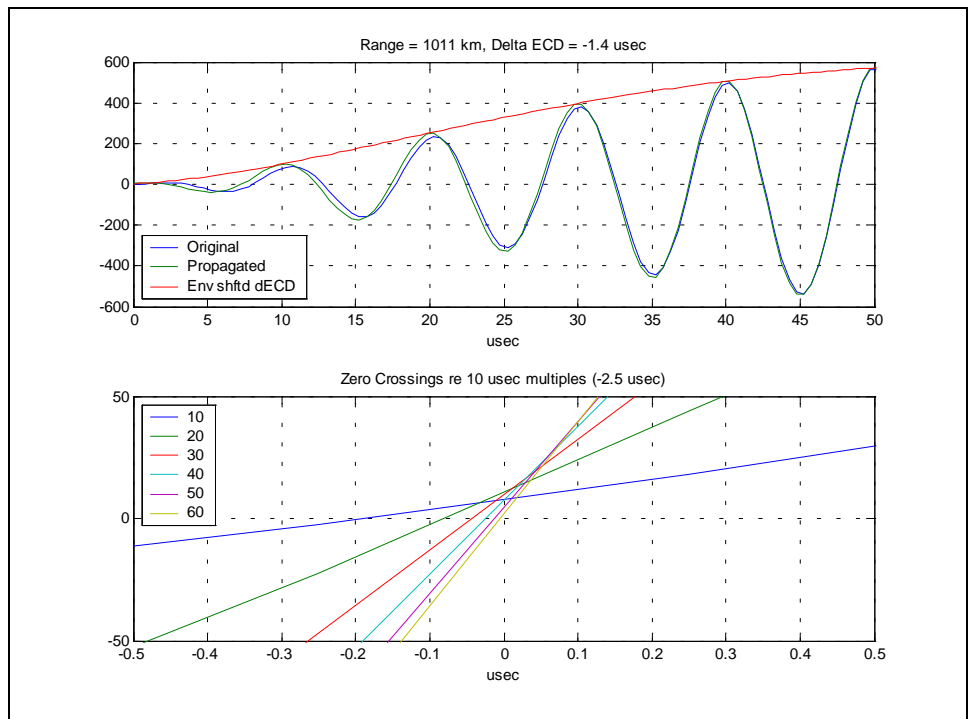


**Fig. 23 – Beyond 1000km zero-crossings continue to disperse in same direction.**

Fig. 21, 22 and 23 show analyses of zero-crossings of distorted pulses derived by Peterson from results. Fig. 21 shows the signal close to the transmitter; the lower plot shows the timings of the 10, 20, 30, 40, 50 and 60 $\mu$ s zero-crossings. The 60 $\mu$ s crossing is used as the time reference and the figure shows the changes of timing of the other crossings with respect to it. In Fig. 22 the pulse is 760km from the

transmitter. The timings of the crossings have become almost uniform. By 1000km (Fig. 23) the crossings have continued to move apart.

The significance of this approach is that, rather than publishing ECDs that tell receiver manufacturers the position of the 3<sup>rd</sup> zero-crossing with respect to that of the envelope, it might be more valuable to publish zero-crossing such as this. However, there may turn out to be a unique correlation between the position of the zero crossings of the pulse and the ECD value.

## 7 ASFs and ECDs Beyond 1000km

When we first started predicting ASFs using the Monteath computation of the integral equations developed by Johler and Berry at the US National Bureau of Standards [19] we observed an interesting effect. Fig. 24 shows the phase delay variations predicted along a 1700km path using the method. The ground conductivity is 8mS/m and there are no terrain variations.

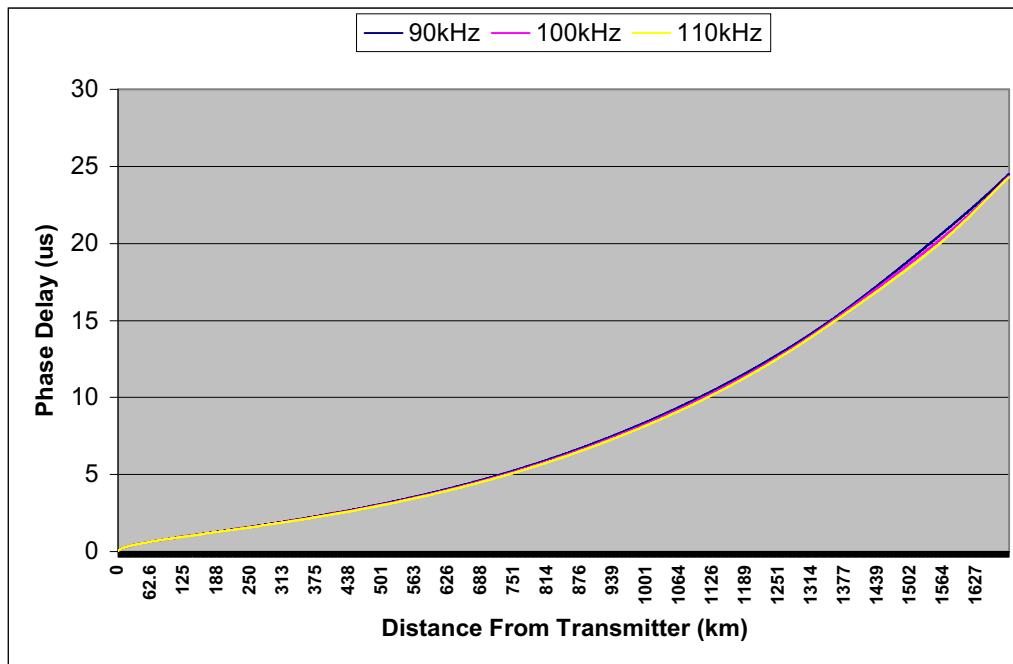


**Fig. 24 – Phase delay (with respect to plane perfectly-conducting earth) with range from transmitter.**

Fig. 25 shows the ASF profile of the path obtained by subtracting the corresponding phase values over sea-water at each point along the path. Beyond about 1000km there are unexpected fluctuations of ASF with range. Since these could not be explained at the time the ASF plots for NELS to publish were computed, their range was limited to 1000km.

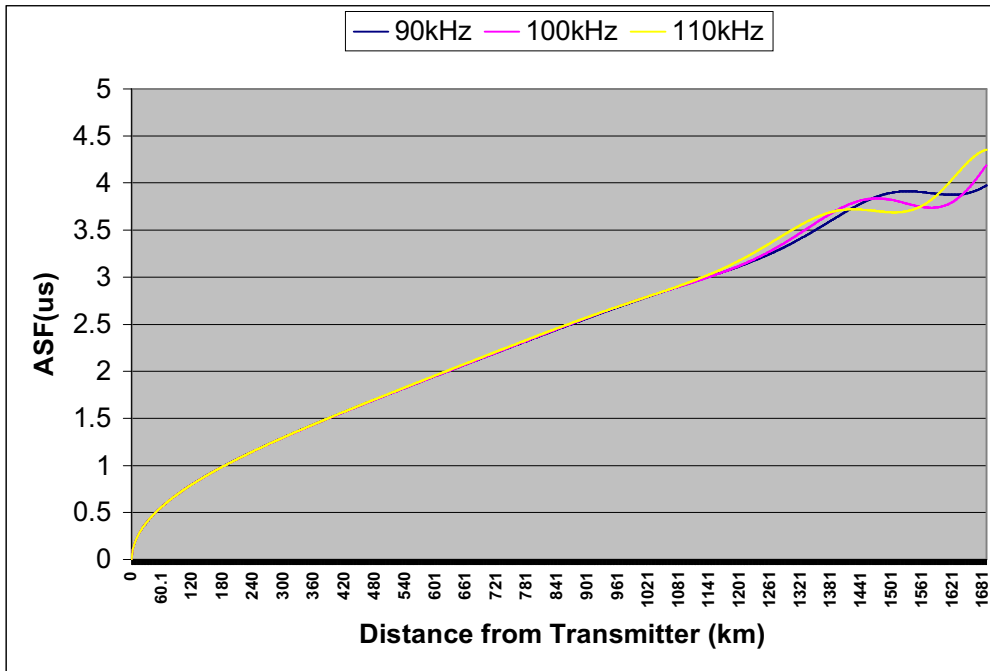


**Fig. 25 – ASF values computed for the smooth earth profile.**

The effect was traced back to Johler and Berry’s equations. It appears that the ASF fluctuations are a standing-wave effect caused by interference between signal components that have followed diffracted ray paths around the bulge of the earth. That is, at long range, the curvature of the earth acts as a very wide and relatively-low hill. This kind of fluctuation is to be seen in Johler and Berry’s own results, downstream of all hills modelled using their equations. The spatial wavelengths of their fluctuation vary with signal frequency, as do ours (Fig. 25). We now believe that our method is predicting ASFs correctly beyond the 1000km range.

These relatively small fluctuations in phase delay at long range are greatly magnified when ECDs are predicted, since ECD depends on small differences in phase velocity with frequency. Fig. 26 shows the consequences: ECD values vary by some  $1.5\mu\text{s}$  over 400km.

## 8 Future Work

Future work on this programme should include comparison of the model results with measured data. We should also study how best to define the ECD of a distorted pulse and whether to publish pulse shape, or zero-crossings, data. Finally, we would like to look for experimental evidence of the long-range fluctuation seen in the Johler and Berry model.

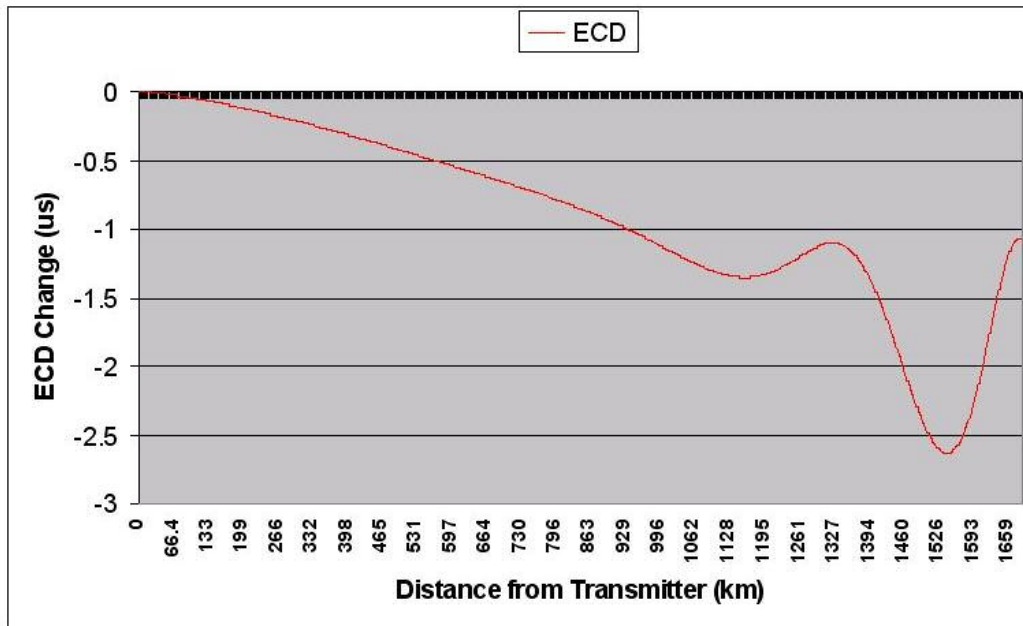


**Fig. 26 – ECD fluctuations at long range.**

## 9 Summary and Conclusions

ECD is a difficult parameter to analyse. It changes with range because of subtle, non-linear, frequency-dependent, variations of both attenuation and phase velocity across the spectrum of the Loran-C signal. Both these factors also vary non-linearly with distance from the transmitter, and are affected by terrain elevation and ground conductivity. All this complexity has been built into the propagation model introduced in this paper.

A good knowledge of ECD is important to maximise receiver integrity. And although we can predict the shapes of received pulses with some confidence, it is not yet clear how best to derive ECD values from them – or whether that is the best way to use the shape information at all!

### Acknowledgements

The authors would like to acknowledge the United States Federal Aviation Administration for funding this work through contract number FAA DFTA 01-01-C-00071 via a sub-contract from Ohio University; and Dr. David Diggie at Ohio University for support. In addition, we would like to thank Dr. Ben Peterson of Peterson Integrated Positioning for the use of his diagrams for Figs. 21, 22 and 23.

## 10 References

- [1] Recommendation ITU-R P.832-2 – World Atlas of Ground Conductivities
- [2] Defence Mapping Agency Product Specifications for World Vector Shoreline, First Edition, 1988, DMA Hydrographic/Topographic Center, Washington, DC
- [3] Performance Specification Digital Terrain Elevation Data (DTED), Project MCGT-0194, Document MIL-PRF-89020A, 1996, National Imagery and Mapping Agency, Bethesda, Maryland, USA
- [4] Specification of the Transmitted Loran-C Signal, United States Coast Guard, Department of Transportation, COMDTINST M16562.4, 1994.
- [5] US Coast Guard, An Analysis of the envelope-to-cycle discrepancy in the Loran-C System, Rep. CG-163-31, Electronic Eng. Div., Apr. 1961.
- [6] Dean, W.N., ECD Variations in Overland Propagation, Proc. 8<sup>th</sup> Ann. Tech. Symp., pp172-185, Wild Goose Association, 1979.
- [7] Sherman, H.T., Finally – a Practical ECD Estimating Technique, Proc. 13<sup>th</sup> Ann. Tech. Symp., Wild Goose Association.
- [8] Farnworth, R.G., Loran-C Coverage Prediction in Western Europe, PhD. Thesis, Univ. of Walesm Jan. 1992.
- [9] Peterson, B.B. & Dewalt, K.M., Analysis of Envelope-to-cycle Difference (ECD) in far field, Proc. 21<sup>st</sup> Ann. Tech Symp., pp89-95, Wild Goose Association.
- [10] Last, J.D. & Williams, P., New sources of ASF data for European Loran users, Ortung und Navigation, Journal of the Deutsche Gesellschaft für Ortung und Navigation, 1/2002, pp119-134, 2002
- [11] Last, J.D., Williams, P., Loran-C for European Non-Precision Approaches, 30<sup>th</sup> Annual Convention and Technical Symposium, International Loran Association, Saint Germain-en-Laye, Paris, France, 7-10 October 2001.
- [12] Last, J.D., Williams, P., Peterson, B. and Dykstra, K., Propagation of Loran-C Signals in Irregular Terrain – Modelling and Measurements Part 1: Modelling, 29<sup>th</sup> Annual Convention and Technical Symposium, International Loran Association, Washington DC, Washington USA, 13-15 November 2000
- [13] Last, J.D., Williams, P., Peterson, B. and Dykstra, K., Propagation of Loran-C Signals in Irregular Terrain – Modelling and Measurements Part 2: Measurements, 29<sup>th</sup> Annual Convention and Technical Symposium, International Loran Association, Washington DC, Washington USA, 13-15 November 2000.

[14] Williams, P. & Last, J.D., Mapping the ASFs of the Northwest European Loran-C system, Journal of the Royal Institute of Navigation, 53, 2, pp225-235, May 2000 (Invited)

[15] Johler, J.R., Kellar, W.J. and Walters, L.C., Phase of the Low Radio Frequency Ground Wave, NBS Circular 573, NBS, June, 1956.

[16] Millington, G., Groundwave Propagation Over an Inhomogeneous Smooth Earth, Proc. IEE, ptIII, **96**, p53, 1949

[17] Pressey, B., Ashwell, G. & Fowler, C., The Measurement of Phase Velocity of Groundwave Propagation of Low Frequencies Over a Land Path, Proc. IEE, **100**, ptIII, p73, 1953

[18] Monteath, G.D., Computation of Groundwave Attenuation Over Irregular and Inhomogeneous Ground at Low and Medium Frequencies, BBC Report 1978/7, British Broadcasting Corporation, Research and Development, Kingswood Warren, Tadworth, Surrey, UK, March 1978.

[19] Johler, J.R., *et. Al.* Loran-D Phase Corrections Over Inhomogeneous Irregular Terrain, Report ITSA 56, Institute for Telecommunication Sciences and Aeronomy, Boulder, Colorado, November 1967.

[20] Freese, D.H., Transmitted Envelope to Cycle Difference (ECD): Definition and Control, United States Coast Guard, EE Cen.